Plant-based torsional actuator with memory

2013 Smart Mater. Struct. 22 072001

(http://iopscience.iop.org/0964-1726/22/7/072001)

IOP FTC
IOP PUBLISHING SMART MATERIALS AND STRUCTURES
Smart Mater. Struct. **22** (2013) 072001 (7pp) doi:10.1088/0964-1726/22/7/072001

FAST TRACK COMMUNICATION

Plant-based torsional actuator with memory

Nayomi Plaza[1,2], Samuel L Zelinka[3], Don S Stone[2,4] and Joseph E Jakes[1]

[1] Forest Biopolymer Science and Engineering, USDA Forest Service, Forest Products Laboratory, Madison, WI 53726, USA
[2] Materials Science Program, University of Wisconsin-Madison, Madison, WI 53706, USA
[3] Durability and Wood Protection Research, USDA Forest Service, Forest Products Laboratory, Madison, WI 53726, USA
[4] Department of Materials Science and Engineering, University of Wisconsin-Madison, Madison, WI 53706, USA

E-mail: jjakes@fs.fed.us

Received 21 December 2012, in final form 30 April 2013
Published 28 May 2013
Online at stacks.iop.org/SMS/22/072001

Abstract
A bundle of a few loblolly pine (*Pinus taeda*) cells are moisture-activated torsional actuators that twist multiple revolutions per cm length in direct proportion to moisture content. The bundles generate 10 N m kg^{-1} specific torque during both twisting and untwisting, which is higher than an electric motor. Additionally, the bundles exhibit a moisture-activated, shape memory twist effect. Over 70% of the twist in a wetted bundle can be locked-in by drying under constraint and then released by rewetting the bundle. Our results indicate that hemicelluloses dominate the shape fixity mechanism and lignin is primarily responsible for remembering the bundle's original form. The bundles demonstrate proof of a high specific torque actuator with large angles of rotation and shape memory twist capabilities that can be used in microactuators, sensors, and energy harvesters.

(Some figures may appear in colour only in the online journal)

1. Introduction

Existing torsional actuators have tradeoffs between specific torque, angle of rotation, reversibility, and environmental constraints that limit their use in ambient conditions. Recent examples of high specific torque actuators that can rotate multiple revolutions per cm length, but not reversibly, include carbon nanotube yarns in electrolyte solutions [1] and wax-filled carbon nanotube yarns [2]. Actuators with less than 4° per cm length rotation have been constructed using piezoelectric materials [3, 4], conjugated polymers in electrolyte solutions [5], and shape memory alloys [6, 7]. If available, a high specific torque actuator that can reversibly rotate large angles could be used for energy harvesters or sensing applications, especially if it also exhibits shape memory twist behavior.

Here we show that bundles of a few wood cells (figures 1(A) and (B)) can be used as moisture-activated torsional actuators capable of reversibly delivering at least two revolutions per cm length at a high specific torque. Furthermore, they possess shape memory twist behavior. Although other researchers have suggested using wood and other lignocellulosic materials as inspiration for stimuli-responsive actuators [8, 9], previous researchers only studied small, unidirectional movements such as the opening of pine cones [10], wheat awn movements [11], and bending of leaning tree organs [12].

Wood possesses a structural hierarchy ranging from individual cellulose microfibrils to cells to growth rings [13].

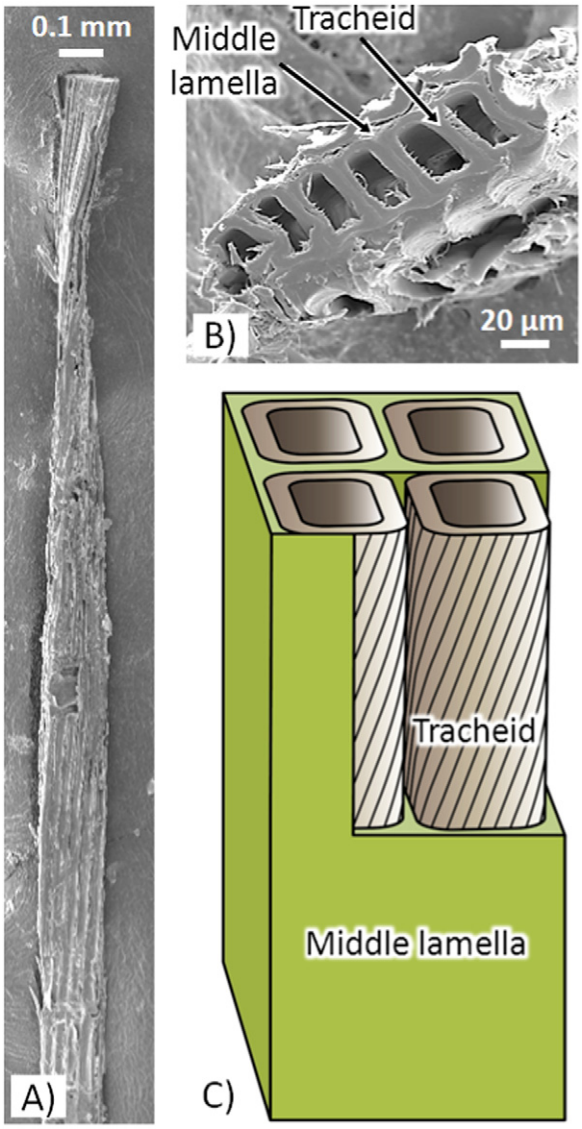

Figure 1. Scanning electron microscope images of a (A) side view of a partially twisted bundle and (B) bundle cross-section. (C) Illustration of a wood cell bundle consisting of tracheids with helically wound cellulose microfibrils held together by the middle lamella.

In softwood, the most common cell is the axial tracheid, typically 30–50 μm in diameter and 3–5 mm in length. The tracheid is hollow with nano-fiber-reinforced composite walls of highly oriented, semicrystalline cellulose microfibrils embedded in a matrix of amorphous cellulose, hemicelluloses, and lignin. Cellulose is a linear polysaccharide, hemicelluloses are branched amorphous polysaccharides, and lignin is a cross-linked amorphous aromatic polymer. From a solubility parameter viewpoint [14], lignin and cellulose are incompatible, but the molecular-level architecture of wood overcomes this by using hemicelluloses to bridge between the cellulose microfibrils and lignin, thus allowing the stiff microfibril reinforcement to be efficiently incorporated into the more compliant lignin and hemicelluloses matrix. In wood, individual cells are held together by the middle lamella (figure 1(C)), which consists of about 20% hemicelluloses

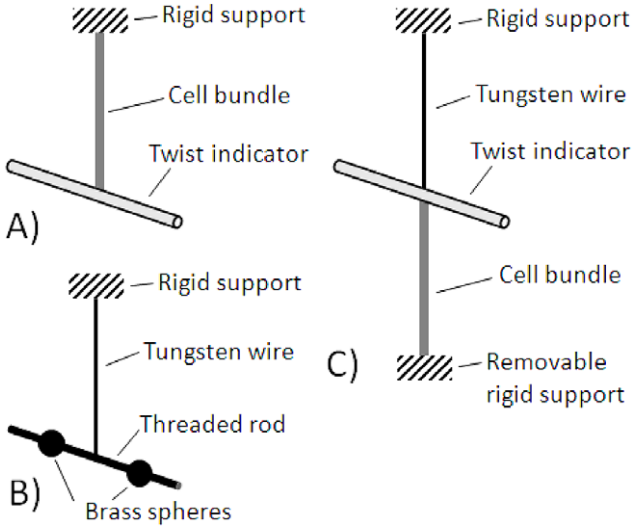

Figure 2. Illustrations of (A) cell bundle twist indicator, (B) torsional pendulum for calibration of a tungsten wire torque sensor, and (C) configuration for measuring bundle torque during moisture-induced twisting and untwisting.

embedded as an irregular, interconnecting network in a matrix of lignin. Another substantial component of wood is water, which is readily absorbed by hemicelluloses [15] and lignin [16]. Moisture content (MC) in wood, defined as water mass divided by oven-dried wood mass, depends on temperature and relative humidity (RH). Up to MC of approximately 30%, called the fiber saturation point, all water in wood is bound by intermolecular attractions within the wood cell walls [17]. At MCs above the fiber saturation point, free water forms in wood cavities.

2. Materials and methods

2.1. Bundle and twist indicator construction

Bundles of a few wood cells were extracted from loblolly pine (*Pinus taeda*) latewood. First, 50 μm-thick longitudinal–tangential sections were cut with a disposable microtome blade fit into a sled microtome. Under a dissecting microscope, hand razors were then used to separate out individual bundles. Scanning electron microscopy images of bundles post-experiment showed that despite efforts to align bundles with the longitudinal tracheid axis, they deviated by approximately 5°–20° from axis. Bundle dimensions ranged from 1 to 2.5 cm in length, with a rectangular cross-section of 50 μm in the narrow dimension and 100 to 150 μm in the wide dimension (figure 1(B)). Typically, a bundle cross-section contained 3–10 full cells. Twist indicators made of hollow polypropylene tubes, or more commonly known as 'cocktail straws', were attached to one end of the bundles (figure 2(A)). The twist indicators were then hung from the top of a Plexiglas® glove box.

2.2. Moisture-induced bundle twisting

Twisting was induced by directly wetting a bundle with a water droplet protruding from the end of a hypodermic needle

or by changing the RH within the glove box. The RH was controlled either with a water–glycerin bath placed inside the glove box or an InstruQuest HumiSys^{TM} HF (Coconut Creek, FL, USA) RH generator. Dried air (nominally 0% RH) was achieved by flowing air through a column dryer filled with anhydrous calcium sulfate. Both digital movies and time-lapse digital photography were employed to monitor time-dependent bundle twist. Experiments were performed at room temperature. Twist as a function of RH conditioning was obtained first in adsorption and then in desorption. The bundles were conditioned at each RH for 10 h.

2.3. Specific torque

A torque sensor inspired by the sensitive torsional pendulums used by Coulomb [18–20] and Cavendish [21] in their fundamental measurements of the electrostatic force constant and gravitational force constant, respectively, was built to measure the torque generated during bundle twisting and untwisting. A 10.2 cm length of a 63.5 μm diameter tungsten wire from Metal Cutting Corporation (Cedar Grove, NJ, USA) was used. The sensor was calibrated by attaching a series of five masses with known moments of inertia and measuring the resulting natural frequencies of oscillation. The masses consisted of two brass spheres threaded onto a fine threaded brass rod and the moments of inertia were modified by changing the distance between the brass spheres (figure 2(B)). The calibration experiments measured the shear modulus of the wire to within 3% of the known 161 GPa tungsten shear modulus. The torsional spring constant of the wire was 2.5×10^{-6} N m rad^{-1}. To measure torque generated during bundle twisting a wood bundle was fixed to the end of the tungsten wire (figure 2(C)). After conditioning the bundle in dry air, the bundle free end was also fixed to a removable rigid support. The movement of the twist indicator was monitored as the RH increased to 100% to assess twisting torque. The same procedure was followed going from 100% to 0% RH to assess untwisting torque. To calculate specific torque for comparison with other types of torsional actuators the volume of the bundle was estimated using the cross-section area measured from SEM images (similar to figure 1(B)) and the measured bundle length. Then, the mass of the bundle was calculated using the 0.6 g cm^{-3} specific gravity of loblolly pine latewood [22].

2.4. Moisture-activated, shape memory twist

The moisture-activated, shape memory twist effect was studied by first wetting a bundle with a droplet of water and constraining the bundle indicator at full twist while the bundle dried. Then the constraint was released and the bundle rewetted with a water droplet and allowed to untwist freely to its original twist. To assess the twist recovery factor (θ_{rf}) as a function of RH conditioning, two bundles were first conditioned at 3% RH. Then they were wetted with water droplets and at maximum twist the indicators were constrained as the bundles dried and reconditioned to 3% RH. The constraint was then released and the bundles were conditioned at sequentially higher RHs, returning to 3% RH between each step to calculate the shape recovery factor, θ_{rf}, induced by the previous RH condition. The θ_{rf} was defined following [23] as $(\theta_u - \theta_{rec})/\theta_u$, where θ_u is the unlocked twist and θ_{rec} is the recovered twist, which was a function of the RH conditioning.

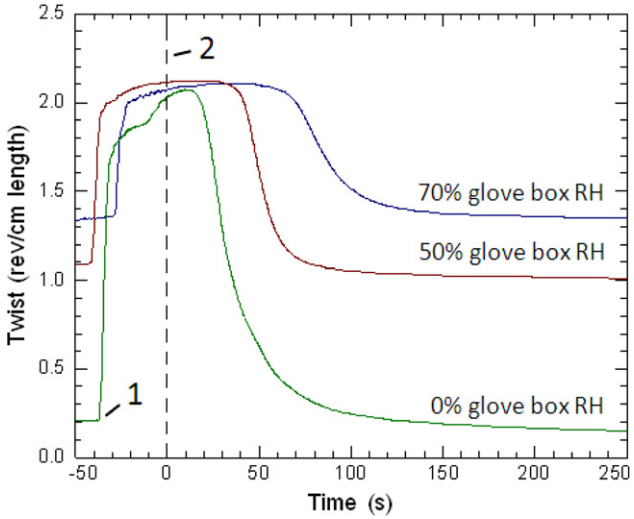

Figure 3. Cell bundle twisting caused by wetting with a water droplet: (position 1) the water droplet touches the cell bundle, causing it to twist; (position 2) the water droplet was removed and the bundle untwists as it reconditions with the glove box RH. Experiments were performed at 0, 50, and 70% RH. The glove box RH was controlled with a water–glycerin bath.

2.5. Moisture-activated, nanoindent recovery

The moisture-activated recovery of nanoindents was studied in both the tracheid wall and middle lamella using surfaces prepared with a diamond knife [24]. The nanoindents were made with a Hysitron TriboIndenter® (Minneapolis, MN, USA) equipped with a Berkovich probe. The nanoindenter chamber was maintained at 35% RH using a water–glycerin bath. Images of residual nanoindents before and after moisture-activated recovery were obtained with a Quesant (Agoura Hills, CA, USA) atomic force microscope (AFM) incorporated in the TriboIndenter® using contact mode.

3. Results and Discussion

3.1. Moisture-induced bundle twisting

A cell bundle begins to twist immediately when touched with a water droplet and continues to twist as the water droplet is moved up and down its length until it is water saturated and no further twisting can occur. After the droplet is removed, the bundle untwists as the bundle MC reconditions with the glove box RH (figure 3). Twisting and untwisting are governed by swelling and shrinkage of the hemicelluloses and lignin constrained by the helically wound cellulose microfibrils. Figure 3 shows experiments performed at 0, 50, and 70% glove box RH. When conditioned at 0%

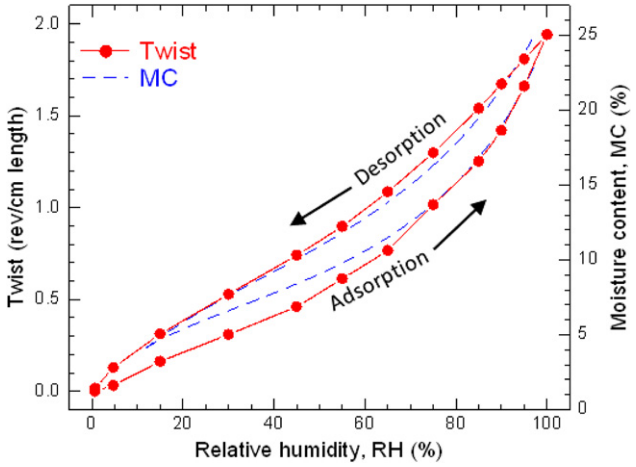

Figure 4. Twist of a cell bundle and moisture content from solid pine [29] as a function of RH. The RH was controlled with an RH generator.

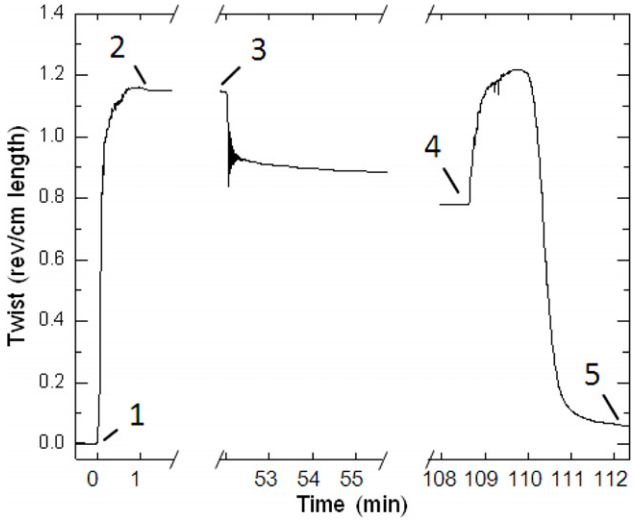

Figure 5. Experiment showing shape memory effect: (position 1) water droplet touches bundle; (position 2) indicator needle constrained during drying; (position 3) indicator needle released; (position 4) bundle rewetted and allowed to twist freely, whereupon it recovers towards its original angle (position 5). The RH was controlled at 60% in the glove box using a water–glycerin bath.

RH the hemicelluloses and lignin are at their lowest MC and have their largest potential to swell during wetting. This is why the largest twist during wetting (2 rev cm^{-1} length) is observed when the cell bundle is conditioned at 0% RH. The bundle twist is substantially less than that observed for an individual cell [25, 26], as expected because the neighboring cells inhibit some of the twist [27, 28]. Nevertheless, the bundles have much higher angles of rotation than actuators constructed from conjugated-polymer systems [5], piezoelectric materials [3, 4], and shape memory alloys [6, 7].

Angular speeds during twisting and untwisting can be assessed from figure 3. However, speeds depend on the moment of inertia of the twist indicator and are therefore properties of the cell bundle twist indicator system and not the cell bundles themselves. The observed maximum angular speed during wetting is 0.2 rev (cm length $s)^{-1}$ in 50 and 70% RH, and 0.3 rev (cm length $s)^{-1}$ in the 0% RH. These speeds are not likely the maximum potential values because twisting speed will depend on how uniformly the bundle can be wetted and a water droplet can only wet a small portion of the bundle at a time. As the bundle reconditions to the glove box RH, the maximum angular untwisting speed of the cell bundle indicator increased with decreasing RH, with values of 0.08, 0.05, and 0.02 rev (cm length $s)^{-1}$ for 0, 50, and 70% RH, respectively. The untwisting speed is likely highest in 0% RH because there is the greatest potential for change in MC, and therefore twist, as the cell bundle dries in 0% RH from the water saturated state.

Bundle twist as function of RH conditioning is shown in figure 4 for both adsorption and desorption. The amount of twist change with RH increases at higher RH. Also, hysteresis is observed between adsorption and desorption. For a given RH, twist is less in adsorption than desorption. The twist data possess a shape and hysteresis that are similar to water sorption isotherms, which demonstrate a direct relationship between twist and MC.

Using our torque sensor (figure 2(C)) we found that a cell bundle produces 6×10^{-7} N m torque during both twisting and untwisting, which results in a 10 N m kg^{-1} specific torque. Compared to other torsional actuators with high angles of rotation, the bundle specific torque is higher than commercial electric motors (up to 6 N m kg^{-1}) [30], carbon nanotube yarn in electrolyte solutions (2.4 N m kg^{-1}) [1], and wax-filled carbon nanotube yarns (8.4 N m kg^{-1}) [2]. Also, the 10 N m kg^{-1} specific torque generated by the bundles during untwisting is an improvement over the carbon nanotube yarn actuators, which must be coupled to torsional return springs to produce high torques during untwisting [1, 2]. The present results suggest an architecture that would obviate the need for external return springs.

3.2. Moisture-activated shape memory effects

A moisture-activated, shape memory twist effect is also exhibited by the bundles (figure 5). This effect is observed by constraining a wetted bundle to prevent it from untwisting during drying. Then, after removing the constraint the majority (about 70%) of the twist remains locked-in. Finally, when the bundle is rewetted, it recovers the locked-in twist. To gain insights into the interplay of cellulose, hemicelluloses, and lignin in the shape memory effect, we study moisture-activated recovery of nanoindents placed in the middle lamella and tracheid wall. A nanoindent in the middle lamella completely recovers after wetting (figure 6) and demonstrates that a composite of lignin and hemicelluloses—without the cellulose fibrils—is a moisture-activated shape memory material. The partial recovery of the nanoindent in the tracheid wall is likely a consequence of the severe, nonrecoverable deformation of the cellulose microfibrils during nanoindentation (figure 6). However, the nearly complete recovery in the shape memory twist experiment (figures 5 and 7) suggests that no permanent cellulose microfibril deformation occurs

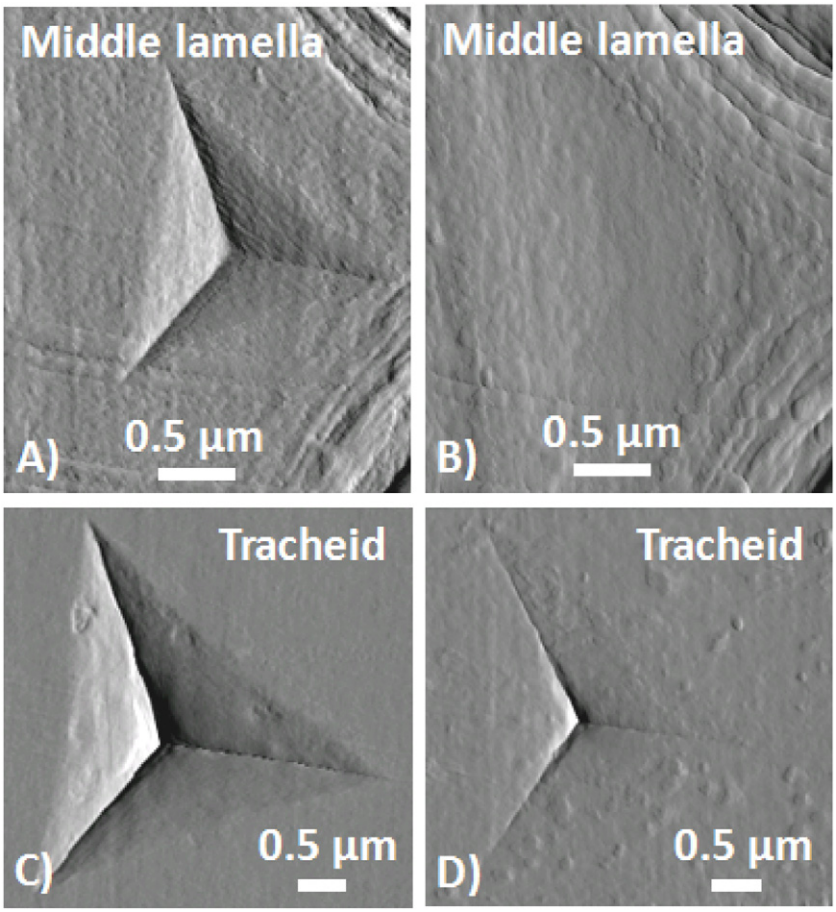

Figure 6. Atomic force microscopy images showing moisture-induced recovery in nanoindents placed in the middle lamella ((A), (B)) and tracheid wall ((C), (D)). Nanoindents were made and imaged dry ((A), (C)). Then the surface was wetted with a drop of water and allowed to dry before reimaging ((B), (D)). The nanoindent in the lignin-rich middle lamella completely recovers, and the nanoindent in the tracheid wall mostly recovers, with the depth decreasing from 410 to 110 nm.

during moisture-induced twisting, in which the strains are much smaller than for the nanoindents.

Because shape memory effects in polymers are usually controlled by property changes at a melting or glass transition (T_g) [31], the behavior of the moisture-dependent T_g of the lignin and hemicelluloses provides insight into the mechanisms controlling the water-activated shape memory effect in the lignin and hemicelluloses composite. Under dry conditions, hemicelluloses and lignin have T_g values well above room temperature, with estimates ranging from 150 to 220 °C and 130 to 200 °C, respectively [32, 33]. Because water acts as a plasticizer, T_g values for hemicelluloses and lignin decrease during water uptake [32–34]. However, only the T_g of hemicelluloses decreases to below room temperature at elevated RH [16, 32–34]. Kelley and coworkers [33] estimated that the T_g of *in situ* hemicelluloses drops below room temperature beginning at about 60% RH. Both Cousins [15] and Olsson and Salmén [34] estimated that the T_g of extracted hemicelluloses drops below room temperature beginning at about 80% RH. In contrast, even water-saturated lignin has a T_g of approximately 70 °C [35].

Hence, we hypothesize that (1) hemicelluloses, whose mechanical properties drastically change as their T_g crosses

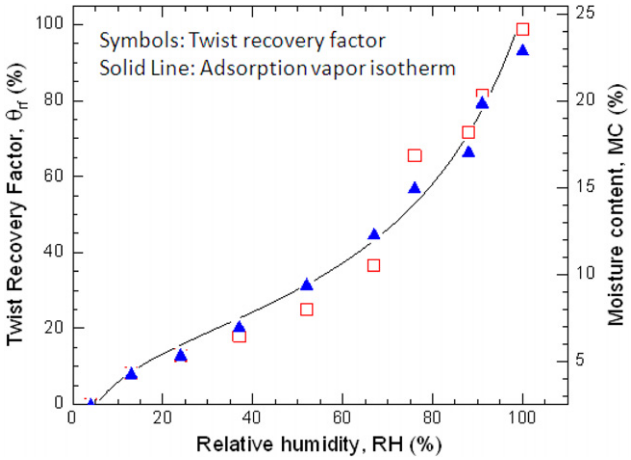

Figure 7. Shape memory twist recovery factor (θ_{rf}) and moisture content (MC) from the adsorption isotherm of solid pine [29] as a function of relative humidity (RH). Each symbol type represents one of two bundles that were tested simultaneously. The θ_{rf} was defined following [23] as $(\theta_u - \theta_{rec})/\theta_u$, where θ_u is the unlocked twist (corresponds to position 4 in figure 5) and θ_{rec} is the recovered twist (corresponds to position 5 in figure 5), which was a function of the RH conditioning. RH was controlled with an RH generator.

room temperature with changing MC, dominate the shape fixity mechanism and (2) lignin, whose T_g remains above room temperature, dominates the recovery mechanism. During moisture-induced twisting, secondary molecular bonds, particularly hydrogen bonds between hydroxyl groups, break and reform within the hemicelluloses softened by the uptake of water. This breaking and reforming of bonds falls in line with the 'Velcro' analogy recently put forth by Keckes *et al* [36] for viscous flow in wood polymers. Eventually, the cross-linked lignin and stiff cellulose microfibrils restrict further swelling and twisting. If the bundle is then dried under a constraint that prevents untwisting, the hemicelluloses will vitrify into a new conformation, and upon release of the constraint the majority of the twist will be locked-in by the stalled kinetics of recovery. When rewetted and dried without constraint the bundle will return to its original twist, primarily because of lignin's ability to remember its original configuration provides the necessary restoration forces.

Based on this hypothesis, twist recovery should predominantly occur above 60–80% RH, which is the RH when the T_g of hemicelluloses drops below room temperature [15, 33, 34]. The dependence of the twist recovery factor (θ_{rf}), which measures the percentage of locked-in twist recovered after conditioning at a given RH, is plotted and compared with the adsorption isotherm in figure 7. Similar to the relationship between twist and MC in figure 4, a direct relationship is observed between θ_{rf} and MC. Indeed, θ_{rf} exhibits an upswing above 60% RH (figure 7), indicating that twist recovery accelerates as the T_g of hemicelluloses falls below room temperature. However, substantial twist recovery also occurs at lower RH. This is likely caused by the complex distribution of hemicelluloses and lignin within the cell walls, which results in a large distribution of relaxation-time spectrum and consequently a large distribution in mechanical softening behavior controlling the twist recovery.

4. Concluding remarks

Bundles of wood cells, or possibly even bioinspired synthetic bundles, provide engineers with new torsional actuators that possess high angles of rotation, high specific torque, and shape memory twist behavior that could be incorporated into the design of smart materials and structures. Recently reported synthetic torsional actuators, such as carbon nanotube yarn [1, 2] and fiber-directed conjugated-polymer systems [5], could be modified to include a shape memory matrix. The material providing the shape fixity mechanism could be activated by any of a variety of external stimuli, including temperature, solvent, moisture, light, or magnetic fields [23, 31, 37]. The synthetic torsional actuators could be used singly or, like our bundles, a bundle of actuators could be engineered to give a prescribed angle of rotation or specific torque.

Acknowledgments

NP acknowledges the SURE-REU program at UW-Madison for providing the initial opportunity to conduct this research during summer 2011 and the GERS program at UW-Madison and 2012 NSF GFRP for graduate support to continue the research. SLZ and JEJ acknowledge PECASE funding. The authors also thank Karen Nelson in the Office of Communications of FPL for the illustration in figure 1(C), Tom Kuster in the Analytical Chemistry and Microscopy Laboratory at FPL for the SEM images in figures 1(A) and (B), and Professors Rod Lakes and Izabela Szlufarska at UW-Madison for manuscript review and helpful discussions.

References

[1] Foroughi J *et al* 2011 Torsional carbon nanotube artificial muscles *Science* **334** 494–7
[2] Lima M D *et al* 2012 Electrically, chemically, and photonically powered torsional and tensile actuation of hybrid carbon nanotube yarn muscles *Science* **338** 928–32
[3] Pan C L, Ma Y T, Liu Y B, Zhang Q and Feng Z H 2008 Torsional displacement of piezoelectric fiber actuators with helical electrodes *Sensors Actuators* A **148** 250–8
[4] Glazounov A E, Zhang Q M and Kim C 2000 Torsional actuator based on mechanically amplified shear piezoelectric response *Sensors Actuators* A **79** 22–30
[5] Fang Y, Pence T and Tan X 2011 Fiber-directed conjugated-polymer torsional actuator: nonlinear elasticity modeling and experimental validation *IEEE/ASME Trans. Mechatronics* **16** 656–64
[6] Prahlad H and Chopra I 2007 Modeling and experimental characterization of SMA torsional actuators *J. Intell. Mater. Syst. Struct.* **18** 29–38
[7] Keefe A C and Carman G P 2000 Thermo-mechanical characterization of shape memory alloy torque tube actuators *Smart Mater. Struct.* **9** 665–72
[8] Fratzl P and Barth F G 2009 Biomaterial systems for mechanosensing and actuation *Nature* **462** 442–8
[9] Burgert I and Fratzl P 2009 Actuation systems in plants as prototypes for bioinspired devices *Phil. Trans. R. Soc.* A **367** 1541–57
[10] Dawson C, Vincent J F V and Rocca A-M 1997 How pine cones open *Nature* **390** 668
[11] Elbaum R, Zaltzman L, Burgert I and Fratzl P 2007 The role of wheat awns in the seed dispersal unit *Science* **316** 884–6
[12] Burgert I, Eder M, Gierlinger N and Fratzl P 2007 Tensile and compressive stresses in tracheids are induced by swelling based on geometrical constraints of the wood cell *Planta* **226** 981–7
[13] Wiedenhoeft A C 2013 Structure and function of wood *Handbook of Wood Chemistry and Wood Composites* ed R M Rowell (Boca Raton, FL: CRC Press) pp 9–32
[14] Hansen C M and Bjorkman A 1998 Ultrastructure of wood from a solubility parameter point of view *Holzforschung* **52** 335–44
[15] Cousins W J 1978 Young's modulus of hemicellulose as related to moisture content *Wood Sci. Technol.* **12** 161–7
[16] Cousins W J 1976 Elastic modulus of lignin as related to moisture content *Wood Sci. Technol.* **10** 9–17
[17] Berry S L and Roderick M L 2005 Plant-water relations and the fibre saturation point *New Phytol.* **168** 25–37
[18] Coulomb C-A 1785 Premier mémoire sur l'électricité et le magnétisme *Histoire de l'Académie Royale des Sciences* (Paris: De l'Imprimerie Royale) pp 569–77
[19] Coulomb C-A 1785 Second mémoire sur l'électricité et le magnétisme *Histoire de l'Académie Royale des Sciences* (Paris: De l'Imprimerie Royale) pp 578–611
[20] Magie W F 1963 Coulomb: law of electric force *A Source Book in Physics* (Cambridge: Harvard University Press) pp 408–17

[21] Cavendish H 1798 Experiments to determine the density of the earth Philosophical *Trans. R. Soc.* **88** 469–526
[22] Cramer S, Kretschmann D, Lakes R and Schmidt T 2005 Earlywood and latewood elastic properties in loblolly pine *Holzforschung* **59** 531–8
[23] Xie T 2010 Tunable polymer multi-shape memory effect *Nature* **464** 267–70
[24] Jakes J E, Frihart C R, Beecher J F, Moon R J, Resto P J, Melgarejo Z H, Surez O M, Baumgart H, Elmustafa A A and Stone D S 2009 Nanoindentation near the edge *J. Mater. Res.* **24** 1016–31
[25] Gillis P P and Mark R E 1973 Analysis of shrinkage, swelling and twisting of pulp fibers *Cellulose Chem. Technol.* **7** 209–34
[26] Stanzl-Tschegg S 2005 Properties of chemically and mechanically isolated fibres of spruce (Picea abies [L.] Karst.). Part 2: twisting phenomena *Holzforschung* **59** 247–51
[27] Gray D G and Kam A 1997 Chiral characteristics of thin wood sections *Holzforschung* **51** 1–5
[28] Schulgasser K and Witztum A 2004 The hierarchy of chirality *J. Theor. Biol.* **230** 281–8
[29] Zelinka S L and Glass S V 2010 Water vapor sorption isotherms for southern pine treated with several waterborne preservatives *ASTM J. Test. Evaluat.* **38** 80–8
[30] Hollerbach J M, Hunter I W and Ballantyne J 1991 A comparative analysis of actuator technologies for robotics *The Robotics Review* vol 2, ed O Khatib, J Craig and P Lozano (Cambridge, MA: MIT Press) pp 299–342
[31] Liu C, Qin H and Mather P T 2007 Review of progress in shape-memory polymers *J. Mater. Chem.* **17** 1543–58
[32] Back E L and Salmén L 1982 Glass transitions of wood components hold implications for molding and pulping processes *TAPPI J.* **65** 107–10
[33] Kelley S S, Rials T G and Glasser W G 1987 Relaxation behaviour of the amorphous components of wood *J. Mater. Sci.* **22** 617–24
[34] Olsson A-M and Salmén L 2003 *The Softening Behavior of Hemicelluloses Related to Moisture* ed P Gatenholm and M Tenkanen (Washington, DC: American Chemical Society)
[35] Salmén L 1984 Viscoelastic properties of in situ lignin under water-saturated conditions *J. Mater. Sci.* **19** 3090–6
[36] Keckes J, Burgert I, Fruhmann K, Muller M, Kolln K, Hamilton M, Burghammer M, Roth S V, Stanzl-Tschegg S and Fratzl P 2003 Cell-wall recovery after irreversible deformation of wood *Nature Mater.* **2** 810–3
[37] Miaudet P, Derré A, Maugey M, Zakri C, Piccione P M, Inoubli R and Poulin P 2007 Shape and temperature memory of nanocomposites with broadened glass transition *Science* **318** 1294–6